Site-Specific Spectral Response of Seismic Movement due to Geometrical and Geotechnical Characteristics of Sites

Behrouz Gatmiri,[a,b,*)] Pouneh Maghoul,[b)] and Chloe Arson,[b)]

[a] University of Tehran, Tehran, Université de Paris Est, institut Navier, Ecole des Ponts, Paris
[b] Université de Paris Est, Institut Navier, Ecole Nationale des Ponts et Chaussées, Paris

Abstract

It is well-known that the response of a site to a seismic solicitation depends on local topographical and geotechnical characteristics. Many aspects of seismic site effect still need to be studied in more detail and they can be incorporated in the seismic norms after quantification. The purpose of this paper is to contribute to establishment of a simple method to include complex site effects in a building code. Horizontal ground movements in various points of 2D irregular configurations subjected to synthetic SV waves of vertical incidence are calculated. The parametric studies are achieved by means of HYBRID program combining finite elements in the near field and boundary elements in the far field (FEM/BEM). The results are shown in the form of pseudo-acceleration response spectra. For the empty valleys, we can classify the spectral response according to a unique geometric criterion: the 'surface/angle' ratio, where surface is the area of the valley opening, and angle denotes the angle between the slope and horizontal line in the above corner. To assess the influence of the two dimensional effect on the spectral response of filled valleys, the response of alluvial basins are compared with the response of one-dimensional columns of soil. Finally, an offset criterion is proposed to choose a relevant computation method for the spectral acceleration at the surface of alluvial basins.

Keywords: building code, seismic site effect, hybrid numerical method, finite elements method, boundary elements method, site specific response spectrum, irregular topography, sedimentary valley, 2D effect, earthquake

1. INTRODUCTION

A seismic site effect manifests itself by the modification of the response of a site subjected to a seismic solicitation in comparison with a reference case. The majority of actual seismic codes rest on the sedimentary effects by using a 1D model. This method allows to measure the influence of nature and thickness of the sedimentary layer on the vertical propagation of the volumic waves. However, these results do not agree with estimates provided by 2D or 3D models.

* Corresponding author.
E-mail addresses : gatmiri@cermes.enpc.fr (B.Gatmiri), maghoulp@lami.enpc.fr (P. Maghoul), arson@cermes.enpc.fr (C. Arson)

Unfortunately, the complete responses of movement taking into account the influence of topographical and geological conditions on seismic movement are not considered in normal engineering practice. This work aims at characterizing and quantifying the combined site effects in the bidimensional configurations, in the spectral domain.

This work considers combined influence of topography and geology on the seismic response of alluvial valleys. The two-dimensional wave scattering is studied with the aid of HYBRID program, combining finite elements in the near field and boundary elements in the far field (FEM/BEM). This program has been developed by Gatmiri and his co-workers ([Gatmiri and Kamalian (2002a); Gatmiri and Kamalian (2002b); Gatmiri and Nguyen (2005); Kamalian et al. (2006)]). The time integration process is optimized in this study by a new time truncation method ([Gatmiri and Dehghan (2005)]). Seismic solicitation is a vertically incident SV Ricker wave. In the following, materials are assumed to be dry and linear elastic. The predominant frequency of the incident signal and the impedance contrast between bedrock and sediment are fixed. The reference site is a station far from the epicentre, which is not subjected to site effects.

In this paper, acceleration response spectra of different empty valleys will be studied. This will help better understanding of the problems encountered in the modelling of topographical effects. Curves will be collected on a unique figure, which will characterize topographical effects in a quantitative and qualitative way in the spectral domain. The influence of bi-dimensionality on the response of the site is studied also. For this purpose, acceleration responses of filled valleys are compared to the responses of one-dimensional column of soil. The height of the 1D reference column is chosen equal to the thickness of the sedimentary layer under the observation point considered on the surface of the filled valley. A civil engineer needs to know how to identify the preponderant site effect in a point of the surface of a given shape. That's why in the latest part of this work, a preponderance criterion is presented.

2. NUMERICAL TECHNIQUE

2.1 FORMULATION OF PROBLEMS COMBINING FE- AND BE- METHODS

In this study, sediments are modelled by finite elements in the near field and substratum media in the far field are modelled by boundary elements. The region of interest is a half-space and thus must be enclosed with fictitious boundary elements known as “enclosing elements”. In the Finite Element formulation, Newton-Raphson iterative technique is used and time discretization is performed by Newmark method. The results are expressed in force and displacement equations, and need to be adapted to the Boundary Element formalism, in which stresses replace forces. This formulation is integrated in HYBRID code and validated in [Gatmiri and Kamalian, 2002a,b]. Two-dimensional fundamental solutions were also found and implemented in HYBRID for saturated porous media ([Gatmiri and Kamalian, 2002b, Gatmiri and Nguyen, 2005]).

2.2 TRADITIONAL TECHNIQUES OF INTEGRATION IN THE DOMAIN IN THE BEM

The boundary integral equation of elastodynamics in time-domain for a homogeneous isotropic elastic medium, occupying a volume Ω, bounded by a surface Γ, and subjected to an incident plane wave, can be written as [Gatmiri and Kamalian (2002a); Gatmiri and Dehghan (2005)]:

$$c_{ij}(\xi).u_j(\xi) = \int_{\Gamma}\int_{t_0}^{t} G_{ij} * t_j(x,t).d\Gamma - \int_{\Gamma}\int_{t_0}^{t} F_{ij} * u_j(x,t).d\Gamma + \int_{\Omega} G_{ij}.F^0.d\Omega\,, \qquad (1)$$

ξ is the source point, x is the field point; u_i and t_i are the amplitudes of the i-th component of displacement and traction vectors, respectively, at the boundary; u_i^{eq} represents the incident wave; the symbol $*$ indicates a Riemann convolution integral; c_{ij} is the discontinuity term depending on the local geometry of the boundary at ξ and on the Poisson's ratio; G_{ij} and F_{ij} are the fundamental solutions representing the displacement and traction at x in direction i due to a unit point force applied at ξ in the j-direction.

In a classic recurrence method, eq.1 can be solved by calculating domain integrals at each new time. Forces defined in the domain are evaluated at nodes or at Gauss integration points. This process has to be repeated for each position of the source point on the boundary, which is rather complicated and time-consuming. The first two equations are:

$$c.u_1 = \int_{\Gamma}\int_{t_0}^{t_1} G_{ij} * t_j(x,t).d\Gamma - \int_{\Gamma}\int_{t_0}^{t_1} F_{ij} * u_j(x,t).d\Gamma + \int_{\Omega} G_{ij}^1.F^0.d\Omega\,, \qquad (2)$$

$$c.u_2 = \int_{\Gamma}\int_{t_1}^{t_2} G_{ij} * t_j(x,t).d\Gamma - \int_{\Gamma}\int_{t_1}^{t_2} F_{ij} * u_j(x,t).d\Gamma + \int_{\Omega} G_{ij}^1.F^1.d\Omega\,, \qquad (3)$$

The Wrobel method requires the storage of all the boundary integral coefficients from the beginning of time discretization to current time. It avoids domain discretization, but requires the storage and manipulation of large amounts of data. CPU time needed for the calculation of forces, from one interval to the next, increases with the number of time iterations. The first equation is the same as (eq.2), and the second one (eq.3) becomes:

$$c.u_2 = \int_{\Gamma}\int_{t_0}^{t_2} G_{ij} * t_j(x,t).d\Gamma - \int_{\Gamma}\int_{t_0}^{t_2} F_{ij} * u_j(x,t).d\Gamma + \int_{\Omega} G_{ij}^2.F^0.d\Omega\,, \qquad (4)$$

2.3 AN OPTIMIZED INTEGRATION TECHNIQUE BY TIME-TRUNCATION

Gatmiri and co-workers have been integrated the optimized time integration process in HYBRID code [Gatmiri and Dehghan, 2005]. The technique lies on time truncation. Integration is limited to a number of time steps (m) chosen at the beginning of the calculation. Consider the case $m=2$. The two first integral equations are the same as in the Wrobel Method (eq.2 and eq.4), whereas the third one is expressed as:

$$c.u_3 = \int_{\Gamma}\int_{t_1}^{t_3} G_{ij} * t_j(x,t).d\Gamma - \int_{\Gamma}\int_{t_1}^{t_3} F_{ij} * u_j(x,t).d\Gamma + \int_{\Omega} G_{ij}^2.F^1.d\Omega\,, \qquad (5)$$

At each step of the calculation, the domain integral can be approximated by generalized mean value theorem applied to the average value of the body force. An iterative process yields to the general formulation of the optimised integration technique. The integration process stops by a convergence criterion based on a small tolerance L_m. Precision is thus, controlled by two parameters: the number of time steps which gives the

backtracking limit (m), and a tolerance coefficient that cuts the calculation when the terms become negligible (L_m). The numerical studies reported in [Gatmiri and Dehghan (2005)] show that the time-truncation process used in HYBRID program is fast and accurate. The minimal meshing size is less than the size required in a traditional integral computation frame. Moreover, artificial waves generated at the truncation points of the model vanish easier if the optimised method is used.

3. TOPOGRAPHIC SITE EFFECTS IN 2D CONFIGURATIONS

3.1 PROBLEM PARAMETERS

In order to give some salient features of topographic effects, various examples that cover different 2D geometries are presented. The configurations of the studied rocky valleys are triangle, trapezium, rectangle, ellipse and truncated ellipse. Valleys are characterized by their half width at the surface and at the base and their depth (figure 1).

For triangular, trapezoidal and rectangular valleys, the angle formed by the slope of the relief relatively to the horizontal line in the above corner is considered, for the ellipsoidal and truncated ellipsoidal configurations, α is the angle between the tangent at the top corner of the valley and the horizontal line.

The values of L_1 for the trapezoidal and truncated ellipsoidal valleys are chosen to be equal to 0,40 and 100m. The value of L for all the valleys equals to 100m. In the present work, simulations are carried out with a depth equal to 20, 40, 60 or 100m. The mechanical parameters of the rocky materials are given in table 1.

3.2 STUDY OF THE TOPOGRAPHICAL EFFECTS IN THE VARIOUS VALLEYS

For a given empty valley, some geometrical points are chosen as stations, in order to study topographical effects. The curves of the acceleration response spectrum are shown for each observation point and for the reference site that is situated on the outcrop. The obtained spectral ratios are also represented. A triplet of curves is thus obtained for every chosen observation point and for every type of valley. For example, these curves for different valleys are shown with H equal to 100 (appendix I). In order to find the more critical point, the curves of the spectral ratio are represented as a function of the adimensional offset variable X / L for the various valleys (figure 2). It can be seen that:

1. In general, for the points whose ordinate is lower than mid-slope point, an attenuation of the acceleration response spectra is observed.
2. In all the valleys, an amplification of acceleration response spectra is observed for all the points located between the station at mid-slope and the upper corner of the valley. The strongest amplification is reached for $X / L = 1$ (i.e. at the edge of the canyon).

Since the spectral ratios at different points for every valley have been studied, it is now possible to quantify attenuations and amplifications of the spectral ratio of a given topography. Figure 3 represents the acceleration response spectra of various canyons for the points located at the following abscissas *X/L= 0, X/L= down edge/slope foot (Down corner), X/L= mid-slop* and *X/L=1(top edge/slope foot (top corner))*. By comparing these curves, the same results can be observed:

1. For all curves, from *X/L= 0* to *X/L= 1*, spectral acceleration tends to increase.

2. An attenuation is observed for *X/L= 0* and *X/L=down edge/slope foot*.
3. The attenuation is transformed into amplification, by going up into slope.
4. Maximum amplification is reached at the point of abscissa *X/L= 1*. This point is the most critical for the seismic analysis. Therefore, afterwards, attention will be focused on the results obtained for this point.

3.3 DOMAIN OF INFLUENCE OF TOPOGRAPHICAL EFFECTS IN EMPTY VALLEYS

If all the acceleration response spectrum curves of the different points of valleys are drawn on a single figure, the domain of influence of topographical effects in empty valleys can be determined (figure 4).

3.4 QUANTIFICATION OF TOPOGRAPHICAL EFFECTS IN EMPTY VALLEYS

As it is observed in the figures 3.d, if the value of *H/L* increases, spectral acceleration increases. If the curves of all studied shapes are compared, it is difficult to find a correlation between the topographical characteristics and the amplification of the seismic response of the site.

3.4.1 NON-CURVED GEOMETRIES (TRIANGLE, TRAPEZIUM AND RECTANGLE)

At first, curves relating to the ellipse and truncated ellipse are not considered (figure 5). Table 2 establishes a relation between the geometrical parameters of the remaining shapes and the classification of the calculated seismic amplifications.

There is a very clear correlation between the parameter 'S/A' (surface/angle) and the classification. It is thus possible to model topographical site effects in the various configurations only by means of that parameter (S/A).

3.4.2 CURVED GEOMETRIES (ELLIPSE AND TRUNCATED ELLIPSE)

Secondly, we study all geometric shapes with a fixed ratio of H/L (figure 3.d). Therefore, the modelling of the topographical site effects for curved shapes (ellipse and truncated ellipse) is then possible. For every value of H/L, the spectral response increases with the parameter of S/A. It is noted that the behaviour of curved forms (ellipse and truncated ellipse) is intermediate: the spectral curves are always located between those of the rectangular valleys and the trapezoidal valleys.

4. TWO-DIMENSIONAL ANALYSIS OF THE RESPONSE OF THE SITE

The aim of this section is to study the influence of 2D effects on the seismic response of filled valleys. Acceleration response of filled valleys will be compared to the responses of one-dimensional columns of soil. The height of the 1D reference column is chosen equal to the thickness of the sedimentary layer underlying the observation point considered in the filled valley. The geometrical characteristics of valleys are displayed in the figure 1. It is assumed that valleys are completely filled by a homogeneous sedimentary layer.

4.1 MECHANICAL PARAMETERS OF THE MATERIALS

In the adopted model, the rocky bed and the alluvial layer are assumed to be homogeneous linear elastic materials. The main parameters of the alluvial layer are given in Tab. 3. The impedance contrast β is equal to 0.31, where:

$$\beta = \frac{\rho_S . c_S}{\rho_R . c_R}, \qquad (6)$$

ρ_S and ρ_R are the volumetric masses of sediment and rock, respectively; c_S and c_R are the shear wave's velocities of sediment and rock, respectively.

4.2 STUDY OF COMBINED EFFECTS (2D) IN THE VARIOUS VALLEYS

For a given filled valley, some of the points at surface are chosen as observation stations to study the combined topographical-sedimentary effects. The curves of acceleration response spectra are drawn for each observation point and for the reference site. The spectral ratio obtained from previous spectra is also represented. A triplet of curves is thus obtained for every chosen observation point and for every type of valley. For example, these curves for different valleys are shown with H equal to 100 (appendix II). In order to study the response of each valley to a given seismic solicitation, the curves of the spectral ratio versus adimensional offset variable *X/L* are shown for the various configurations (figure 6). It is observed that:

1. All curves have two parts. A decreasing part from the central point (*X/L= 0*) to a point whose abscissa is between *X/L= 0.5* and *X/L= 1*, and an increasing part between the intermediate point and the top of the slope *X/L= 1*.

For the first part, it is obvious that as we move away from the central point, amplitude decreases, due a decreasing influence of the sedimentary effect ([Gatmiri and Arson, 2007]). The increasing part of the curve shows the predominance of topographical effects on the slopes covered by sediment. In the central part of the valley, one-dimensional sedimentary effect controls the local response of the site. On the slopes of the sedimentary basin, the presence of alluvium attenuates the predominant topographical amplification.

2. Practically, on all curves, the maximal amplification is reached at the central point of the valley (*X/L= 0*). This point seems to be the most critical. This is why afterwards; combined effects are modelled at the centre of valleys.

Figure 7 represents the spectral acceleration response for the various valleys at the superficial points of abscissas *X/L= 0*, *X/L= down edge/slope foot (down corner)* and *X/L= mid-slope*. By comparing these curves, the same tendencies as those described in the previous paragraph are observed: if we move away from the central point of the valley, the amplitude of spectral acceleration response decreases.

4.3 COMPARISON OF 2D COMBINED AND 1D EFFECTS

As can be seen in figure 7.a, the curves form a very compact group. To have a better understanding of the results, only the seven curves giving the strongest amplifications are considered.

In table 4, the curve denoted “n°1” corresponds to the strongest amplification of spectral acceleration response. In this table, a Height/surface parameter has been used.

It is clear that if the height/surface parameter reduces, amplification increases.

It is important to note that:

$$\frac{H}{S} \propto \frac{1}{L}, \tag{7}$$

In the other hand:

$$\frac{H}{S} \downarrow \Rightarrow \frac{1}{L \uparrow} \Rightarrow L \uparrow \Rightarrow amplification \uparrow, \tag{8}$$

It means that, at a given point *X/L= 0*, when L increases, amplification increases. On the other hand, at a given point *X/L= 0*, if the value of height is fixed, the influence of topographical effects in a filled valley disappears, as the surface width increases. Therefore, combined effects are transformed into 1D geological effect. To illustrate this conclusion, the valleys characterized by the same depth, but at the different surfaces S are compared. In this case, varying S with a fixed height changes the values of L. The curves are shown with 'H' equal to 20 and 100m, which are the minimal and maximal values of height in the present parametric study (figure 8). The same result will be achieved; if ‘S’ increases, the amplification of the spectral response in acceleration at the centre of the valley increases.

One question that remains is: on a point far from topographical effect, if the value of L tends to ∞, do curves representing 2D combined effects tend towards curves characterizing 1D effect?

To answer this question, spectral acceleration responses of filled valleys are compared to the one-dimensional responses of 1D columns of soil (figure 9).

By comparing the different curves, it is founded that on a point far from topographical effect, if the value of 'L' tends to ∞, the curves of combined effect tend to the characteristic curve of 1D effect; and in this point, 1D effect is predominant.

5. CONCLUSION

5.1 DEFINITION OF A CLEAR CRITERION FOR TOPOGRAPHICAL EFFECTS IN AN EMPTY VALLEY

As presented in the sections dealing with topographical effects, the spectral acceleration responses are classified according to a unique geometrical criterion: the ‘surface / angle’ ratio. By using figure 5, and making a regression between the minimal and maximal values of the surface / angle parameter, we can find the spectral responses in acceleration for any valley.

5.2 DEFINITION OF A CLEAR CRITERION FOR THE COMBINED EFFECTS AT THE VARIOUS POINTS ON THE SURFACE OF A FILLED VALLEY

A criterion is proposed to determine the predominant site effect at the surface of a filled valley. According to the sections dealing with topographical effects, the spectral acceleration response is attenuated for all points whose ordinate is lower than mid-slope point. On the other hand, in the section concerning the combined site effects, it was observed that in the central zone (first part), the seismic response was amplified. Therefore, in the central zone, sedimentary effects dominate topographical effects. This result is illustrated on figures 10 and 11.

It has already been noticed that at the centre, the spectral responses related to 2D combined effects tend to the one-dimensional analysis results. In central zone, sedimentary effects are always predominant in the centre of the alluvial valleys.

If topographical effects and geological effects at mid-slope are compared (figure 12), it can be seen that topographical effects are lightly predominant in comparison with geological effects. The mid-slope point is thus a good transition point: from this point, up to the edge of the valley (X/L=1), topographical effects dominate the site response (i.e. the preponderance of site effects is reversed).

In conclusion, in the central zone (from X/L=0 to mid-slope), results provided by one-dimensional analyses can be used to estimate the spectral acceleration response of a filled valley (similar to actual paraseismic codes), and in the lateral zone, the spectral response of the sedimentary valleys can be deduced from the characteristic spectra of topographical effects, shown in the figures of the section concerning the topographical site effects.

REFERENCES

[1] Gatmiri, B., Arson C., Nguyen, Khoa- Van, Seismic site effects by an optimized 2D BE/FE method I. Theory, numerical optimization and application to topographical irregularities, Soil Dynamics and Earthquake Engineering, *in Press*.

[2] Gatmiri, B., Arson C., Seismic site effects by an optimized 2D BE/FE method II. Quantification of site effects in two dimensional sedimentary valleys, Soil Dynamics and Earthquake Engineering, *in Press*.

[3] Gatmiri B, Dehghan K. Applying a new fast numerical method to elasto-dynamic transient kernels in HYBRID wave propagation analysis. In: Proc of 6th Conference on Structural Dynamics (EURODYN 2005). Paris, France, 2005. Millpress, Rotterdam, 1879-1884.

[4] Gatmiri B, Kamalian M. On the fundamental solution of dynamic poroelastic boundary integral equations in the time domain. International Journal of Geomechanics 2002a; 2(4):381-398.

[5] Gatmiri B, Kamalian M. Two-Dimensional transient Wave Propagation in Anelastic Saturated Porous Media by a Hybrid FE/BE Method. In: Proc of the 5th European Conference of Numerical Methods in Geotechnical Engineering. Paris, France, 2002b, 947-956.

[6] Gatmiri, B., Nguyen, K.V., Evaluation of seismic ground motion induced by topographic irregularity, Soil Dynamics and Earthquake Engineering 2007, 27, 183-188.

[7] Gatmiri B, Nguyen K.V, Dehghan K. Seismic Response of Slopes subjected to incident SV Wave by an Improved Boundary Element Approach. International Journal for Numerical and Analytical Methods in Geomechanics, *in press.*

[8] Gatmiri B, Nguyen KV. Time 2D Fundamental solution for Saturated Porous Media with Incompressible Fluid. International Journal of Communications in Numerical Methods in Engineering 2005; 21:119-132.

[9] Kamalian M, Jafari MK, Sohrabi-Bidar A, Razmkhah A, Gatmiri B. Time- Domain Two-Dimensional Site Response Analysis of Non-Homogeneous Topographic Structures by A Hybrid FE/BE Method. International Journal of Soil Dynamics and Earthquake Engineering 2006; 26(8):753-765.

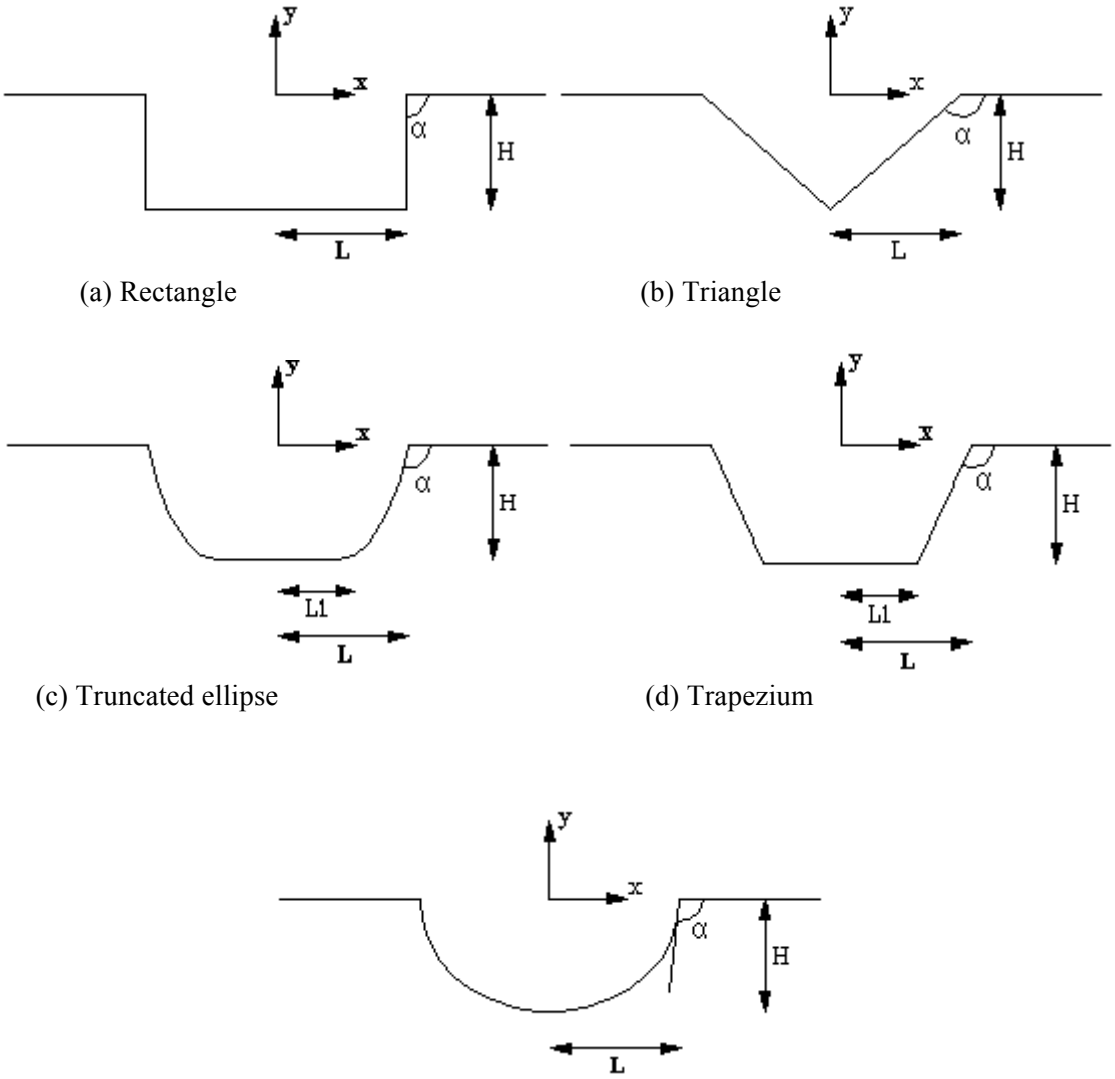

(a) Rectangle (b) Triangle

(c) Truncated ellipse (d) Trapezium

(e) Ellipse

Figure 1. Configurations of the studied valleys

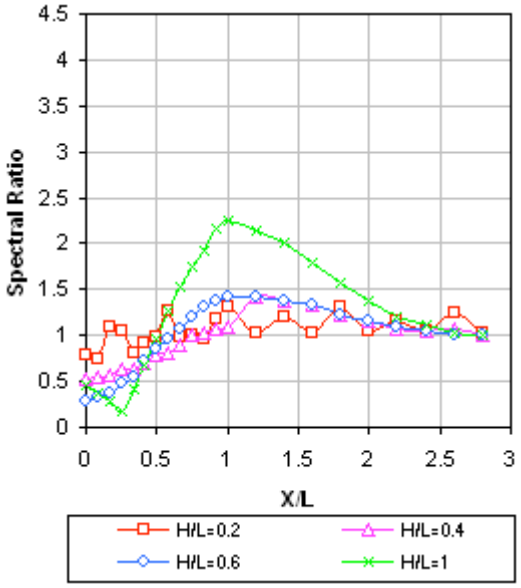

(a) Triangle

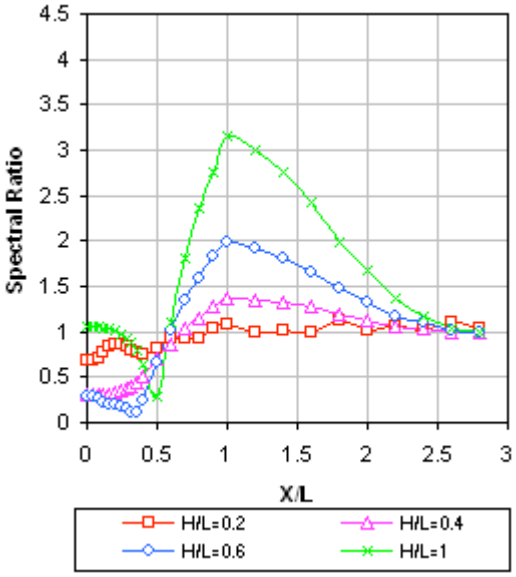

(b) Trapezium

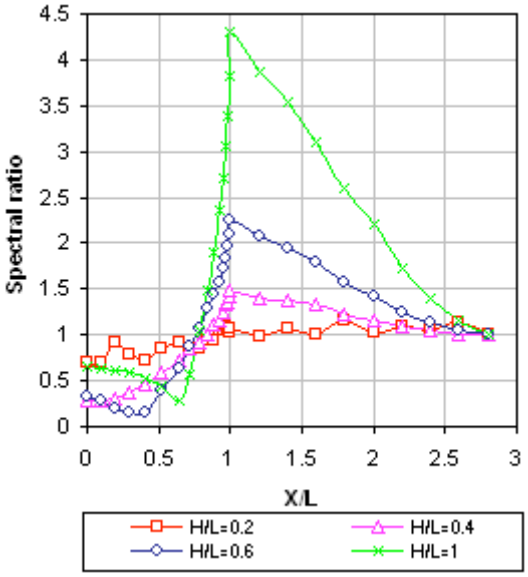

(c) Truncated ellipse

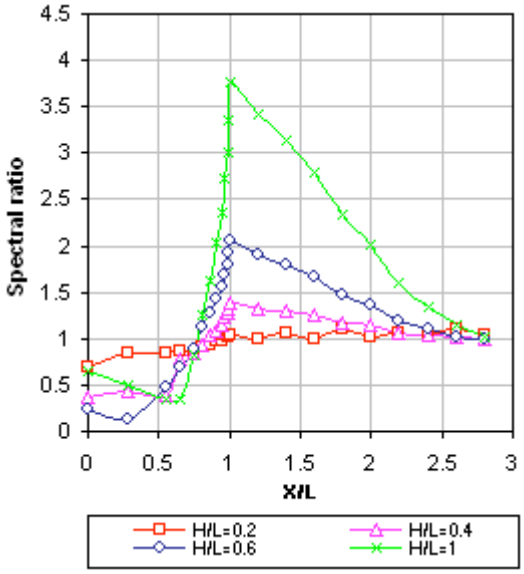

(d) Ellipse

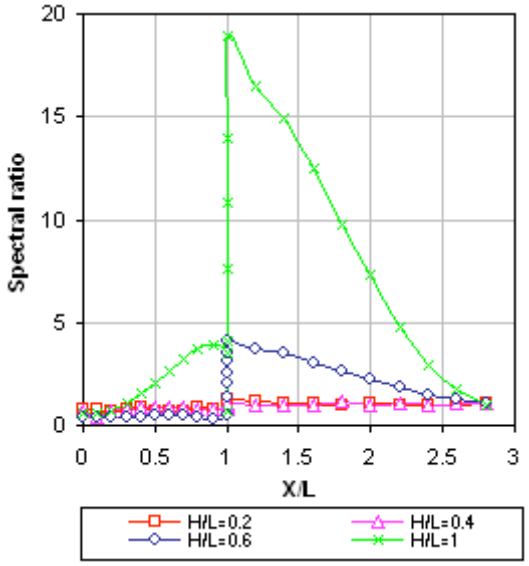

(e) Rectangle

Figure 2. Spectral ratio as a function of adimensional offset variable X / L for the various empty valleys

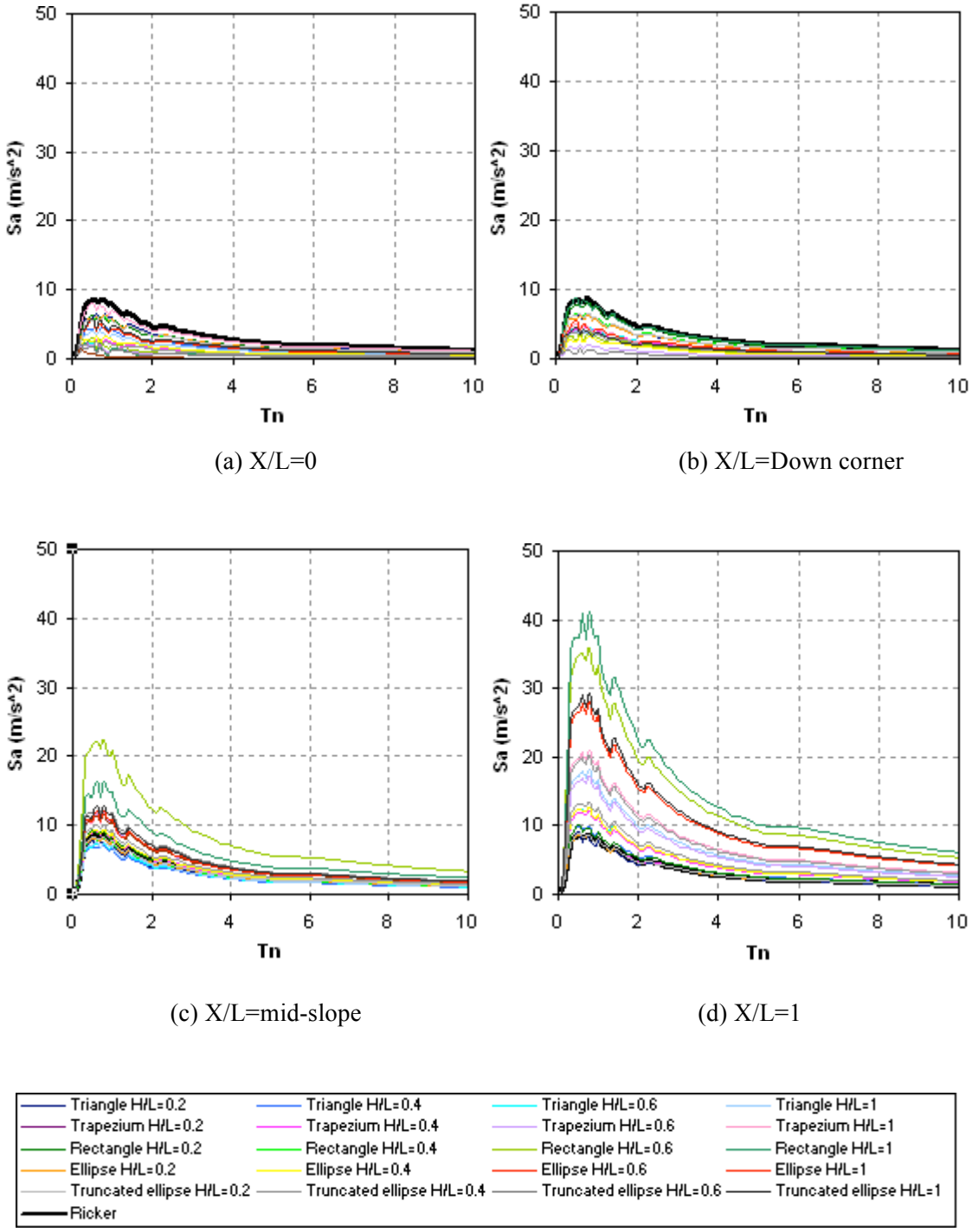

Figure 3. Acceleration response spectra of various valleys a) at X/L= 0, b) at X/L= down edge/slope foot (Down corner), c) at X/L= mid-slop, and d) at X/L=1

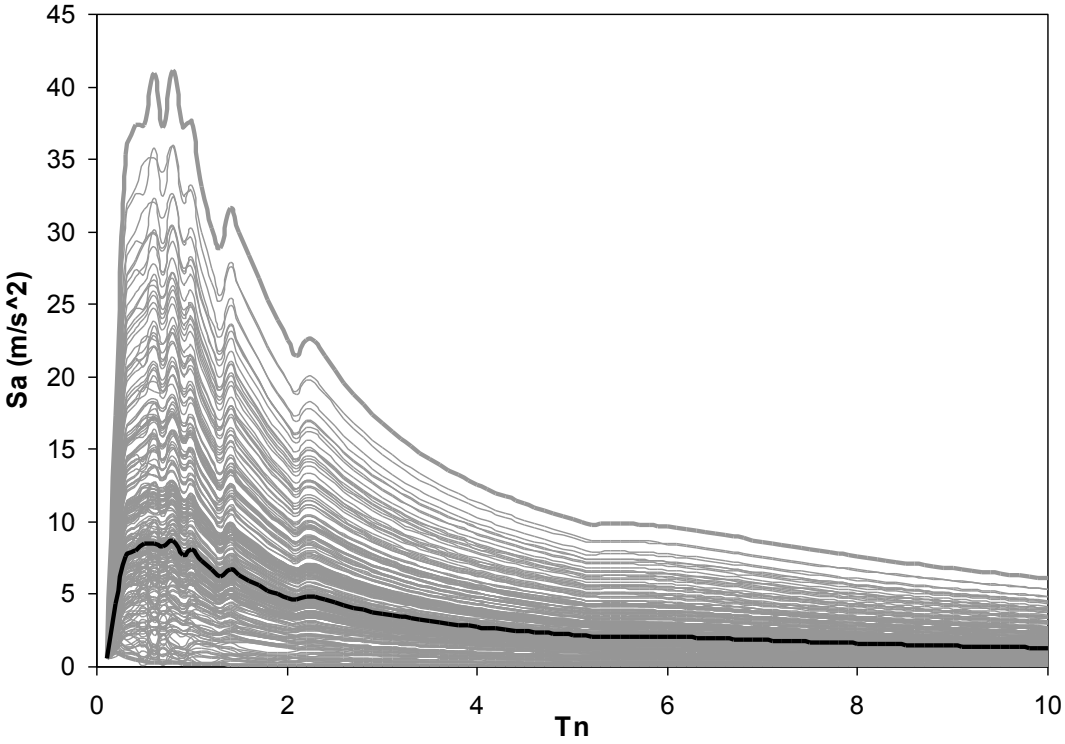

Figure 4. Domain of influence of topographical effects. Black line is the spectrum of Ricker and the grays line are the acceleration response spectra of various observation points of various valleys

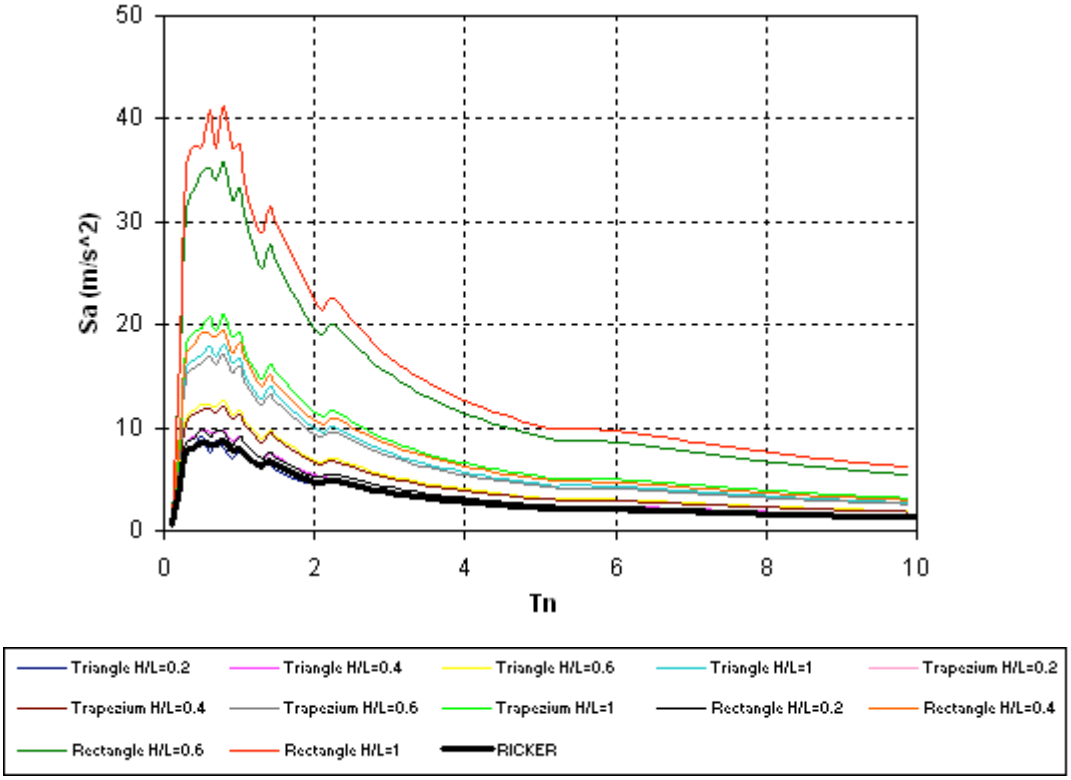

Figure 5. Acceleration response spectra for the various valleys at X / L=1 (top corner)

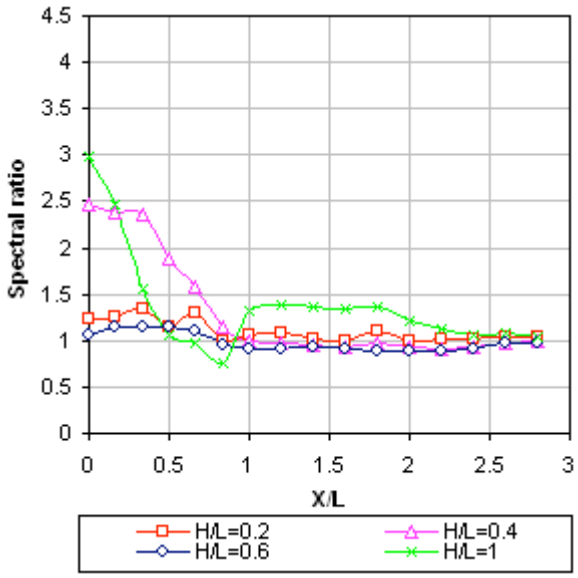

(a) Triangle

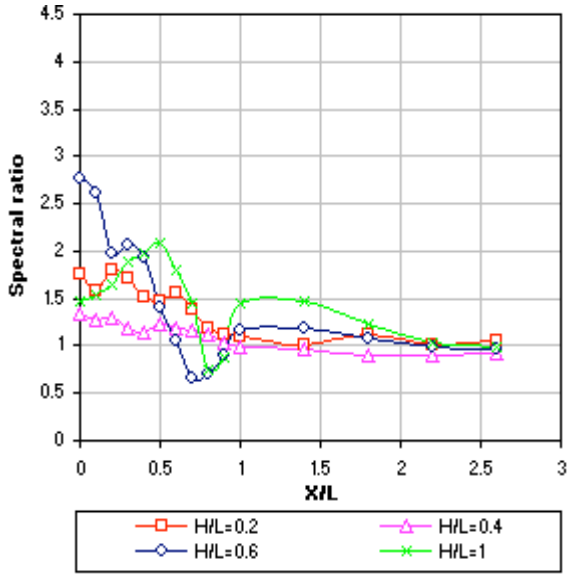

(b) Trapezium

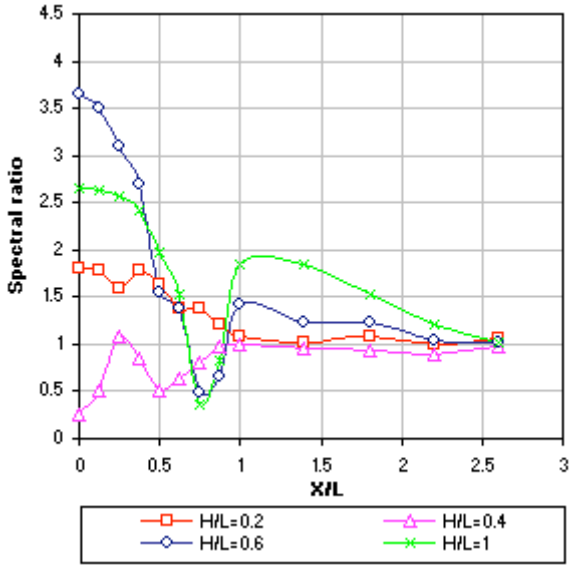

(c) Truncated ellipse

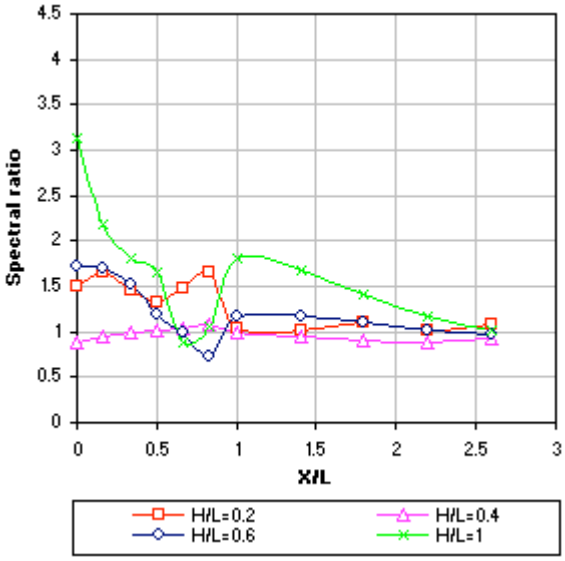

(d) Ellipse

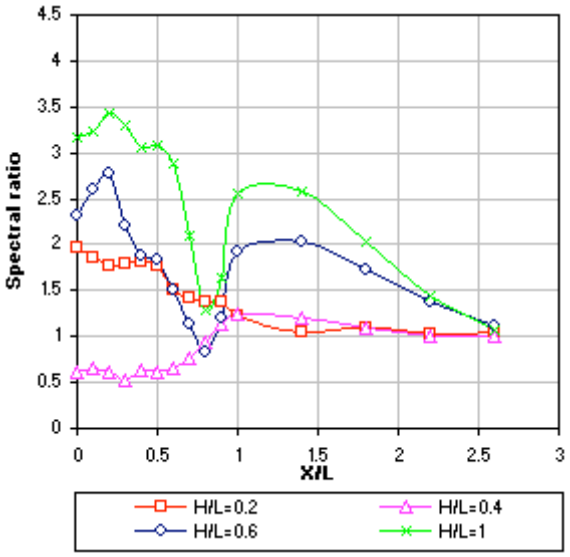

(e) Rectangle

Figure 6. Spectral ratio versus adimensional offset variable X / L for the various empty valleys

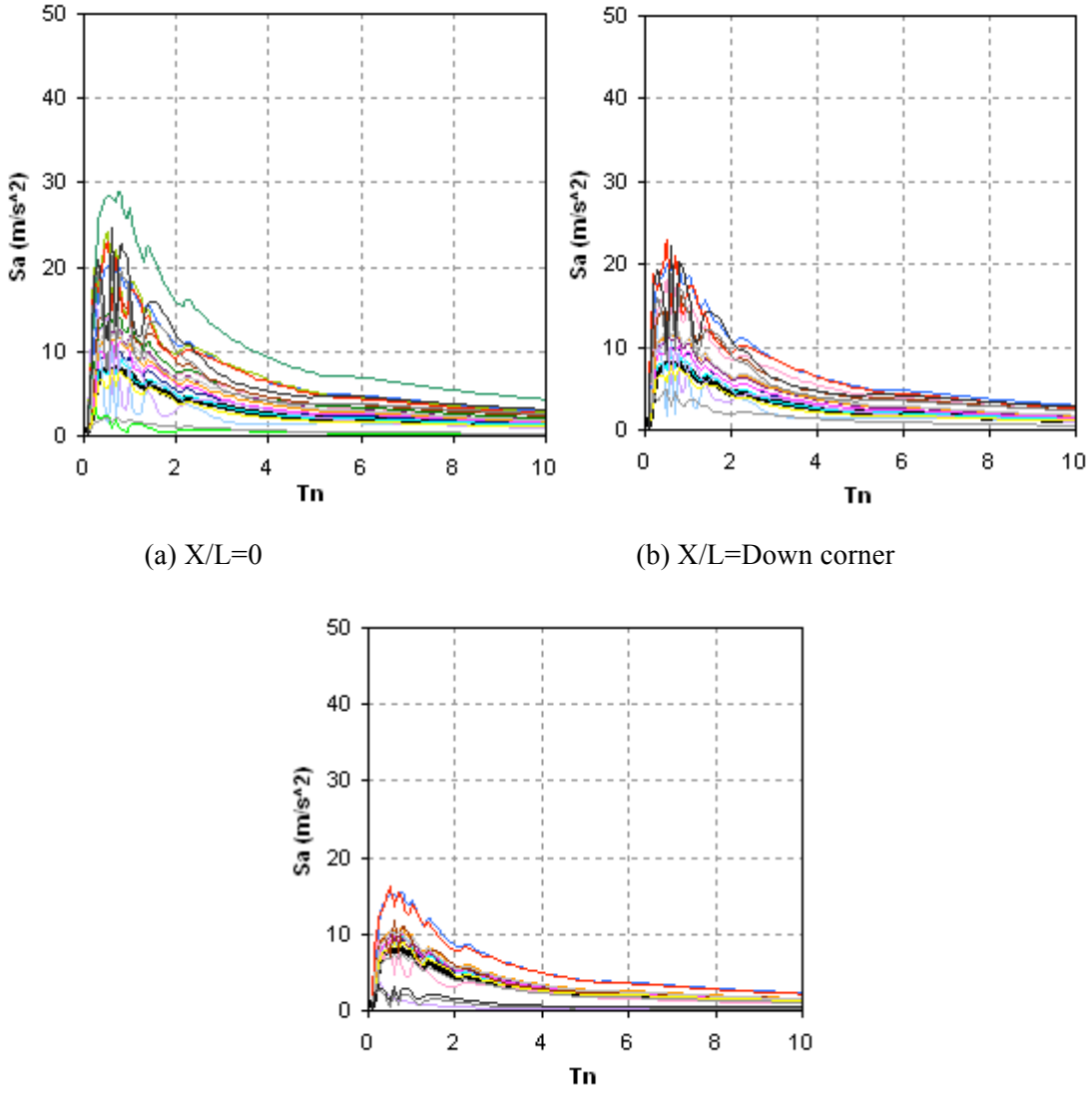

Figure 7. Acceleration response spectra of the various valleys a) at X/L= 0, b) X/L= at down edge/slope foot, c) X/L= at mid-slope

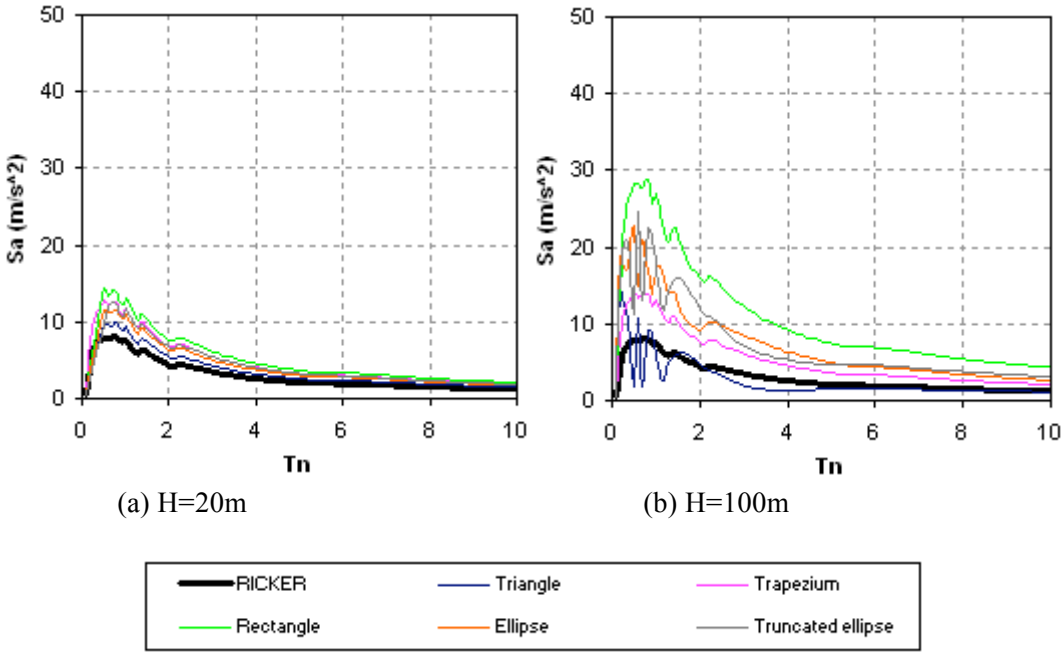

(a) H=20m (b) H=100m

Figure 8. Acceleration spectra of the various valleys at X/L=0, a) H=20, b) H=100

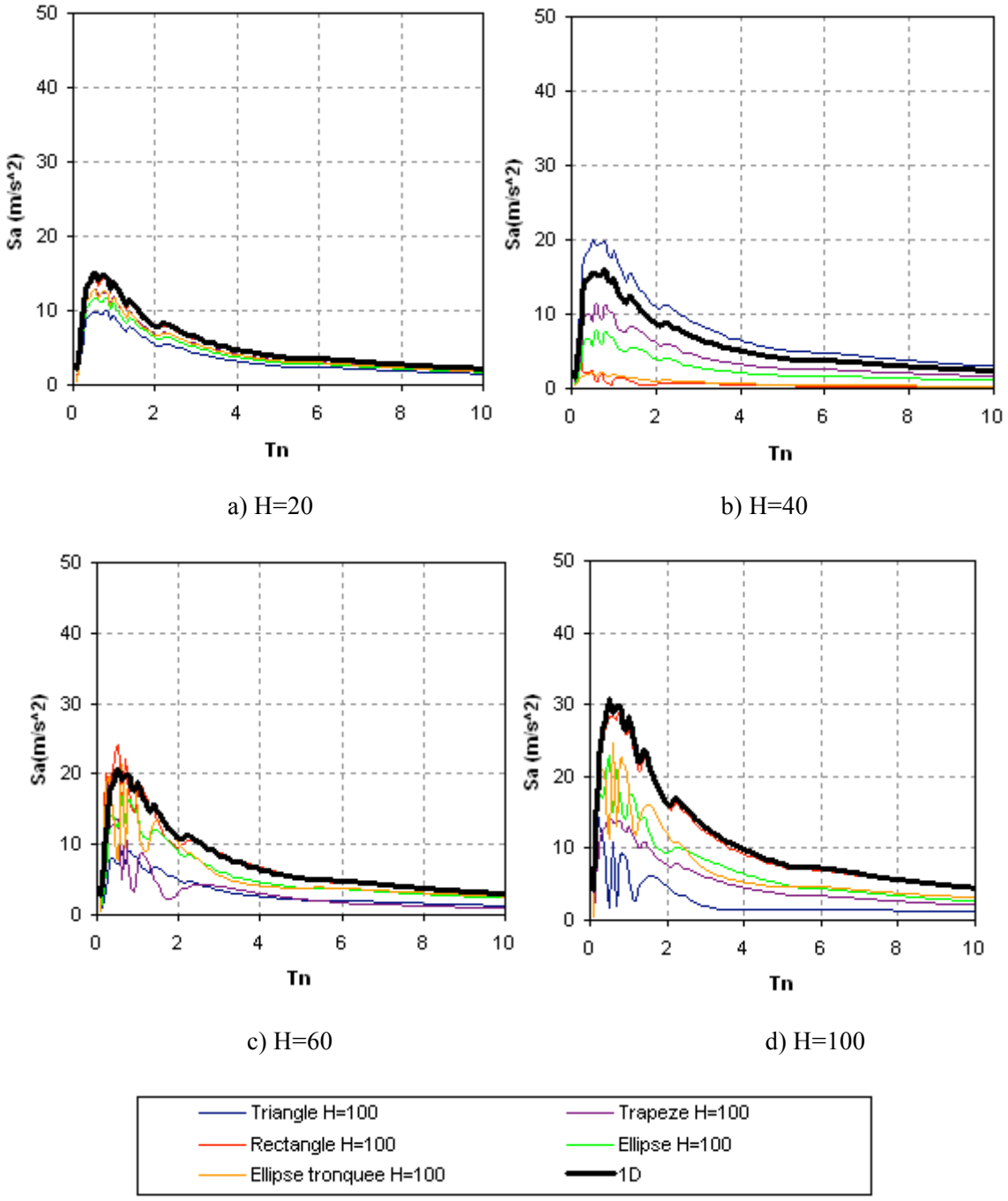

Figure 9. Comparison of the spectral responses in acceleration of full valleys at X/L=0 and the one-dimensional responses of 1D columns of soil, a) H=20, b) H=40, c) H=60, H=100

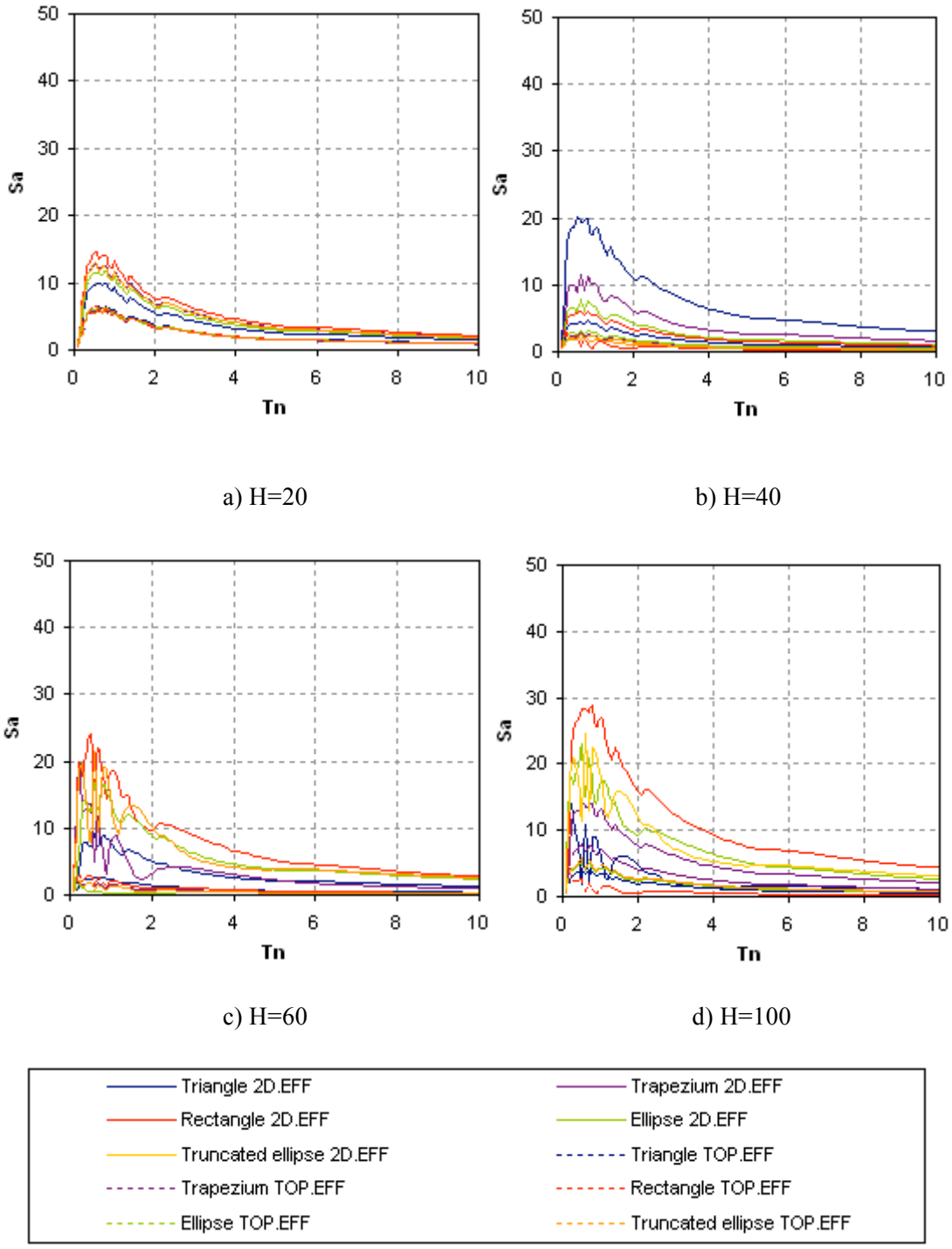

Figure 10. Comparison between the topographical effect in the empty valleys and the combined effect (2D) in the filled valleys at X/L=0, a) H=20, b) H=40, c) H=60, d) H=100

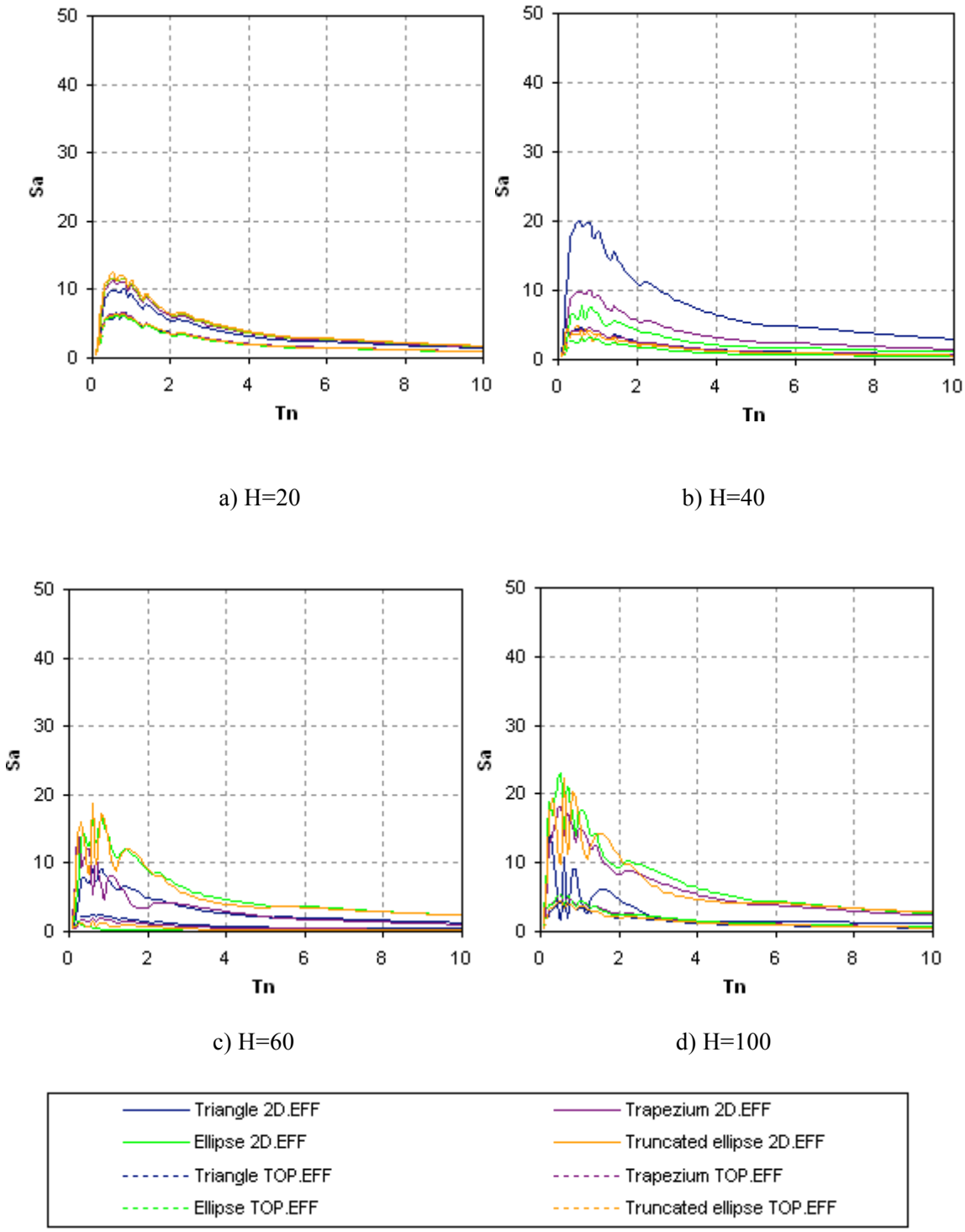

Figure 11. Comparison between the topographical effect in the empty valleys and the combined effect (2D) in the filled valleys at X/L= Corner, a)H=20, b) H=40, c) H=60, d) H=100

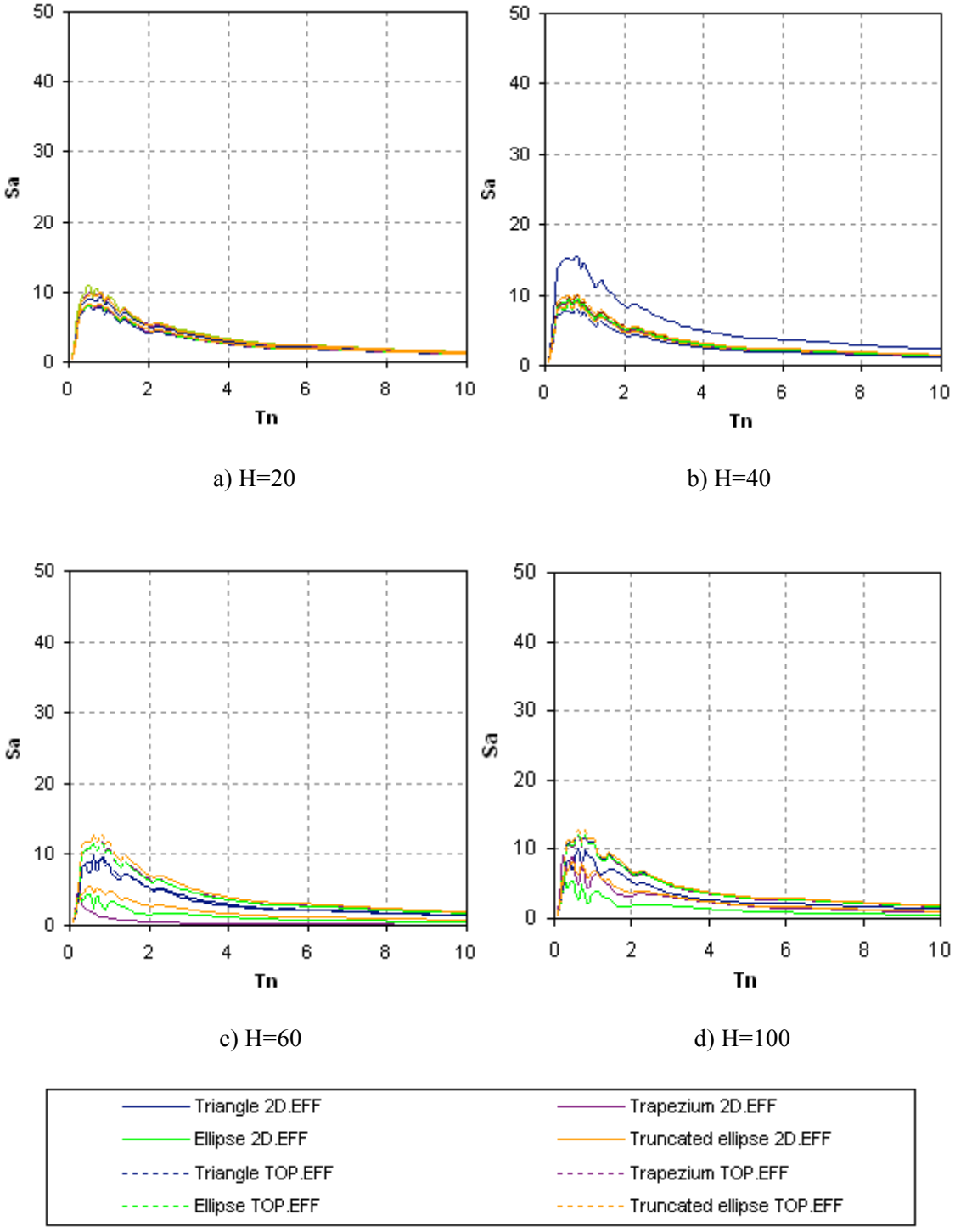

Figure 12. Comparison between the topographical effect in the empty valleys and the combined effect (2D) in the filled valleys at X/L= mid-slope, a)H=20, b) H=40, c) H=60, d) H=100

APPENDIX I

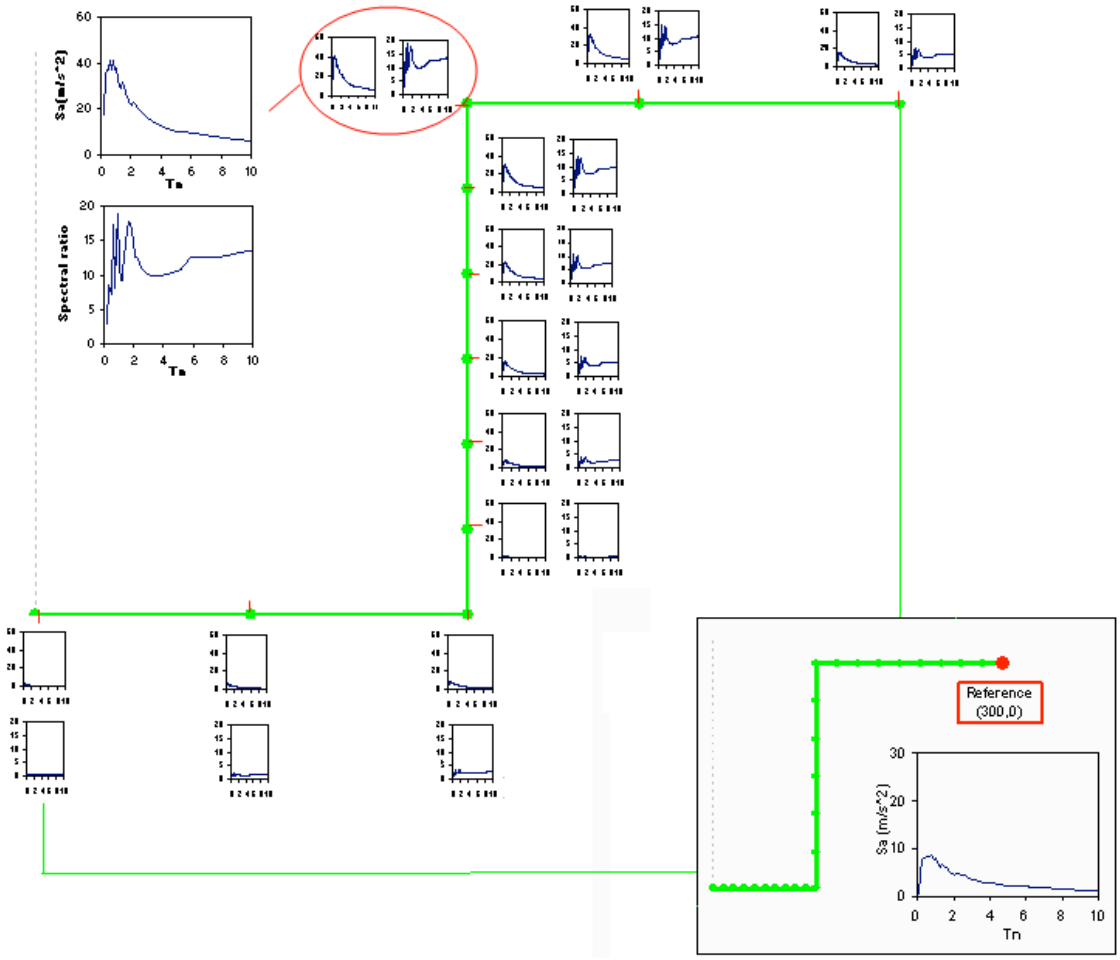

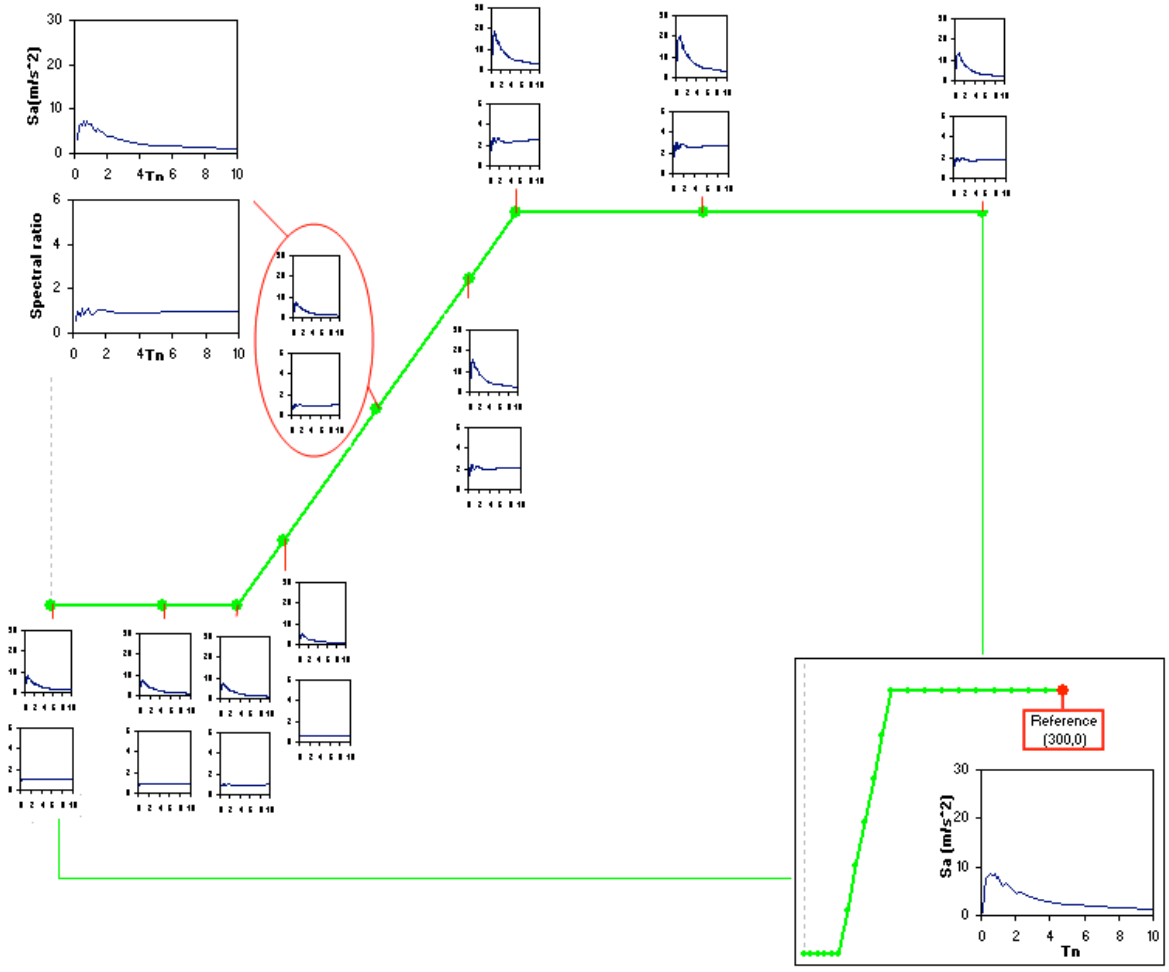
Sa(m/s^2)
Tn
Spectral ratio
Reference
(300,0)
Sa (m/s^2)
Tn

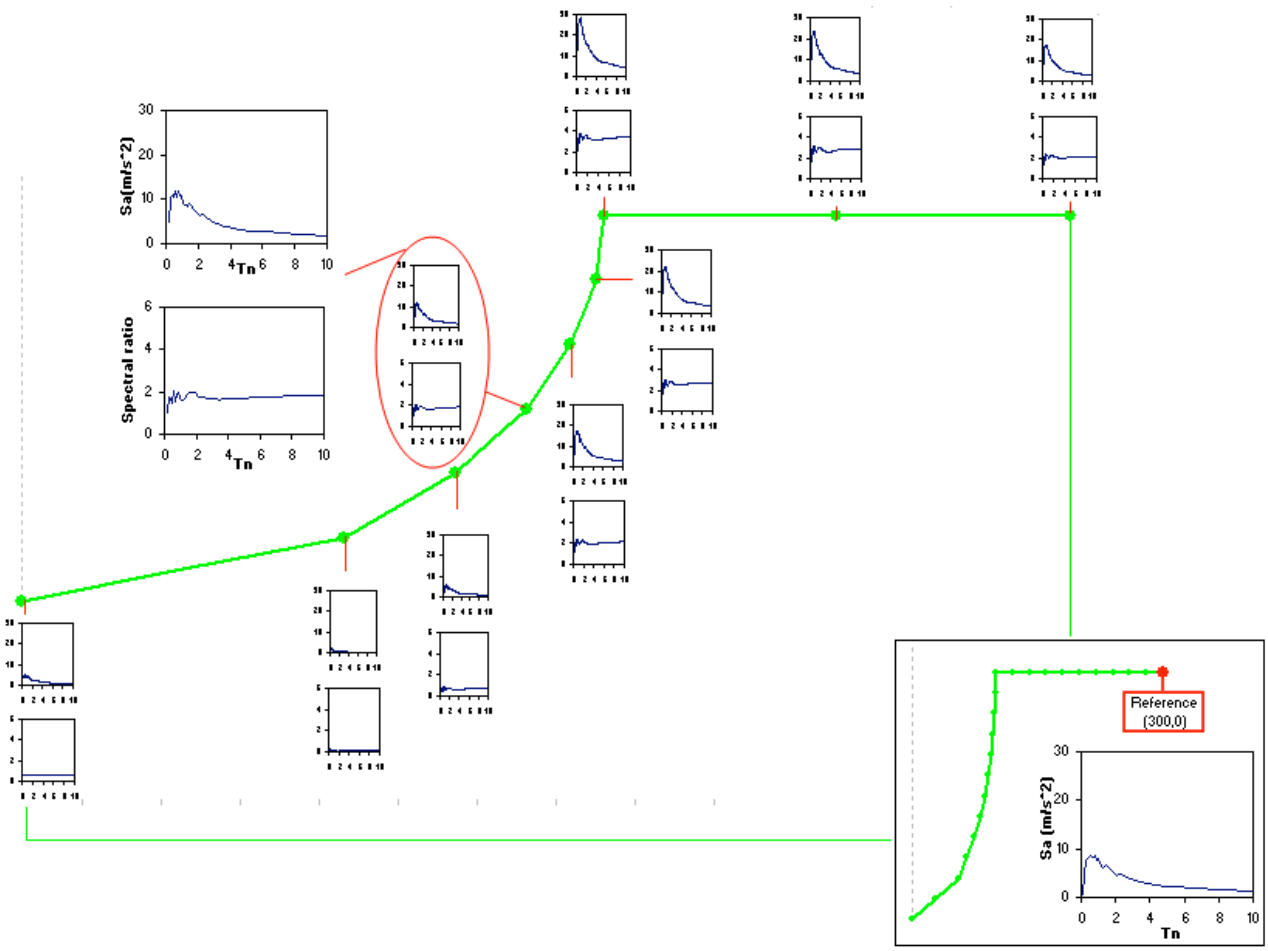
Sa(m/s^2)
Tn
Spectral ratio
Tn
Reference
(300,0)
Sa (m/s^2)
Tn

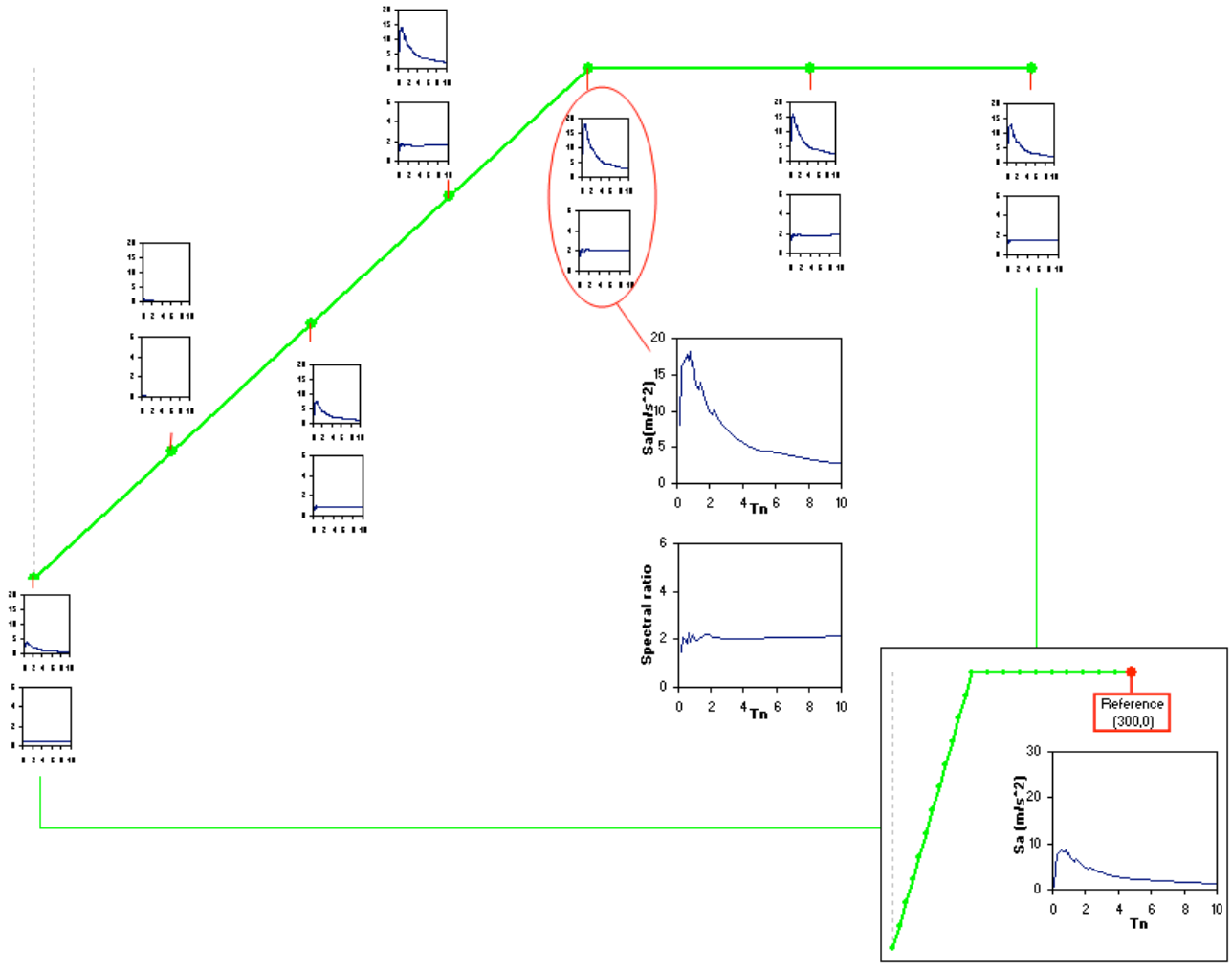
Sa(m/s^2)
Tn
Spectral ratio
Tn
Reference
(300,0)
Sa (m/s^2)
Tn

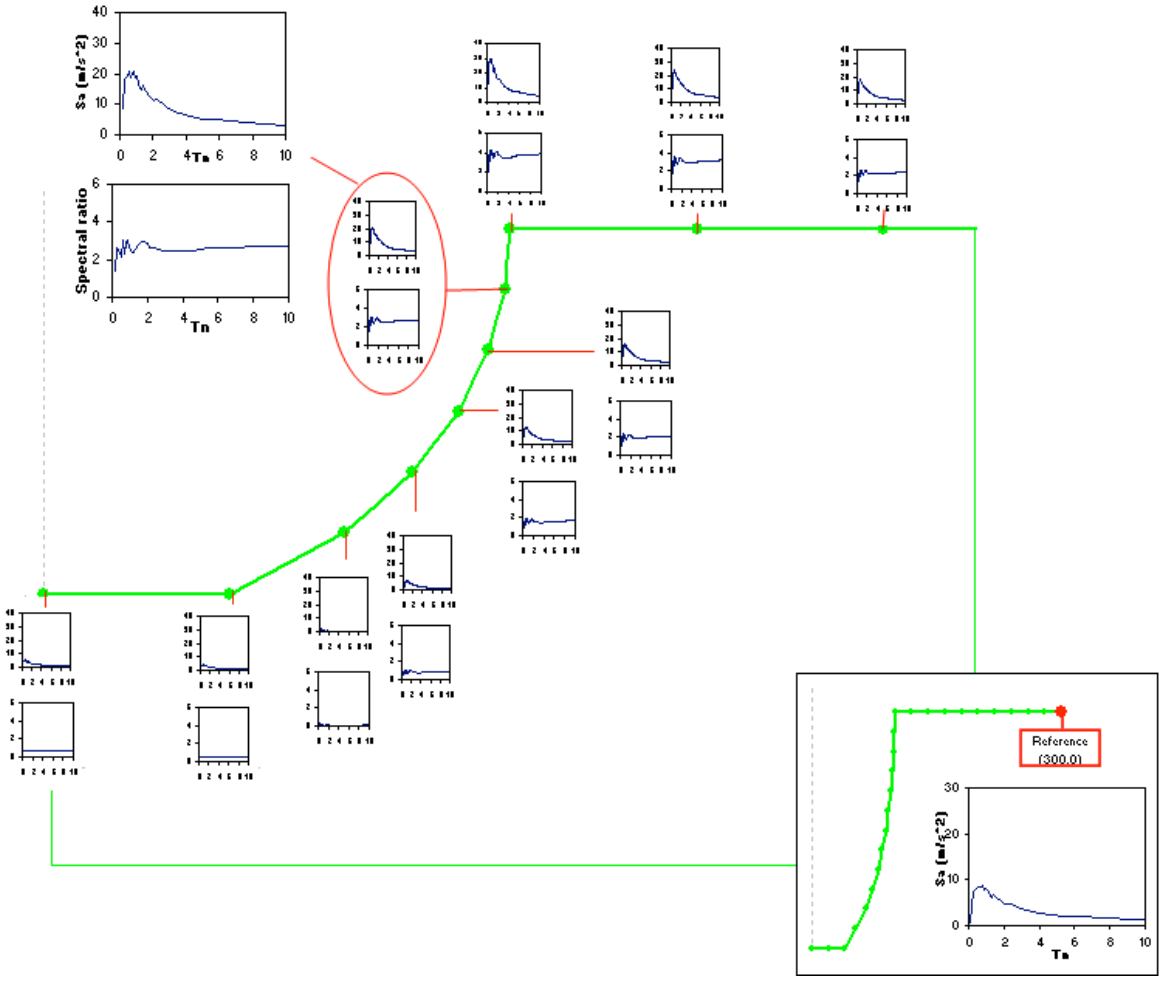
Sa (m/s^2)
Tn
Spectral ratio
Tn
Reference
(300.0)
Sa (m/s^2)
Tn

APPENDIX II

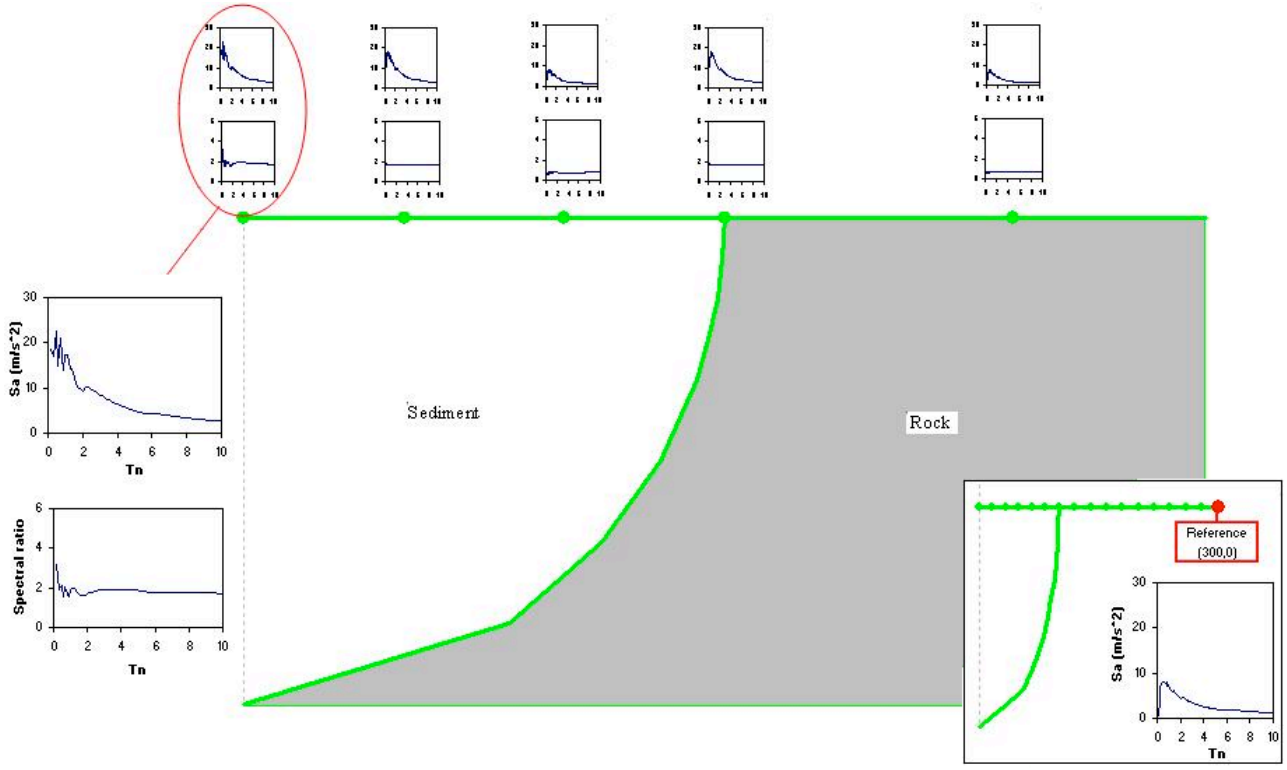
Sediment
Rock
Sa (m/s^2)
Tn
Spectral ratio
Tn
Reference
(300,0)
Sa (m/s^2)
Tn

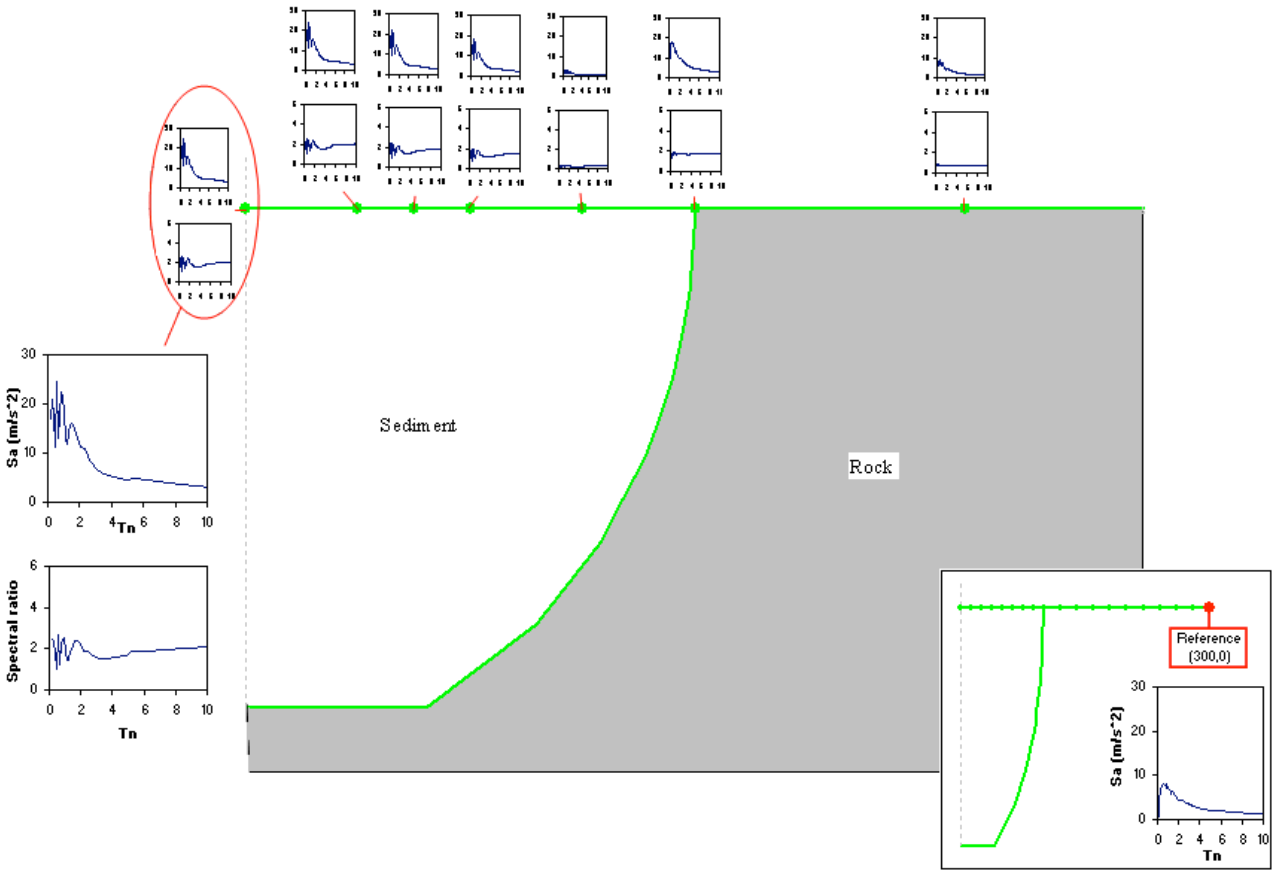
Sediment
Rock
Sa (m/s^2)
Tn
Spectral ratio
Tn
Reference
(300,0)
Sa (m/s^2)
Tn

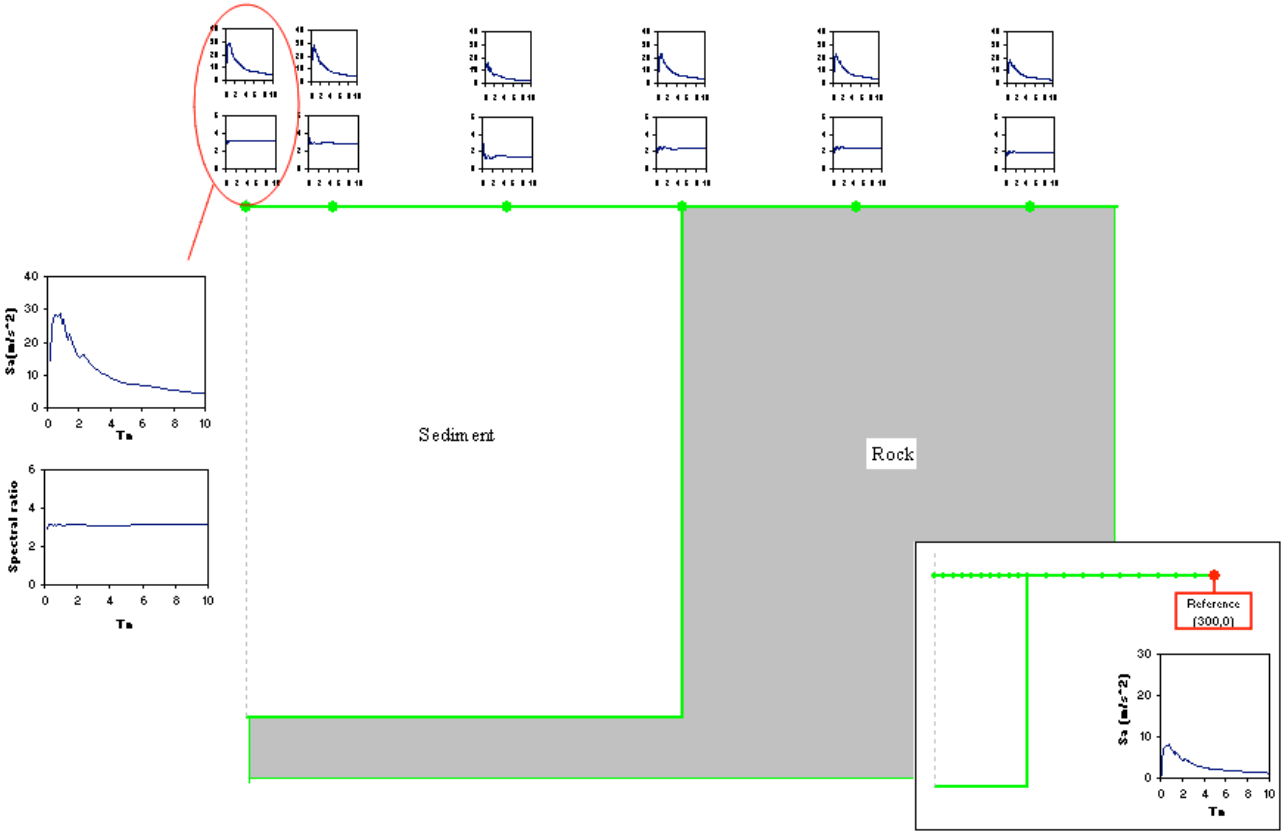
Sa[m/s^2]
Ts
Spectral ratio
Ts
Sediment
Rock
Reference
(300,0)
Sa [m/s^2]
Ts

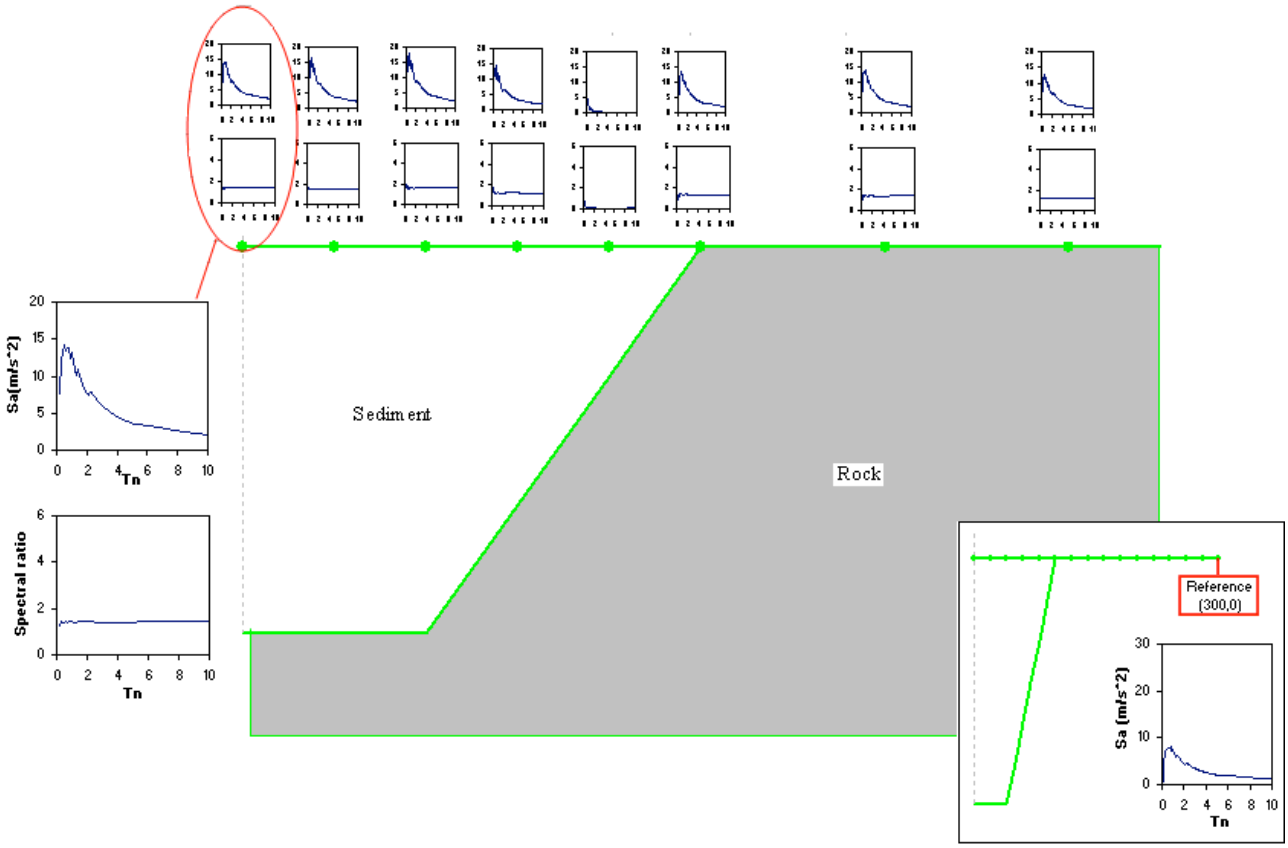
Sa(m/s^2)
Tn
Spectral ratio
Tn
Sediment
Rock
Reference
(300,0)
Sa (m/s^2)
Tn

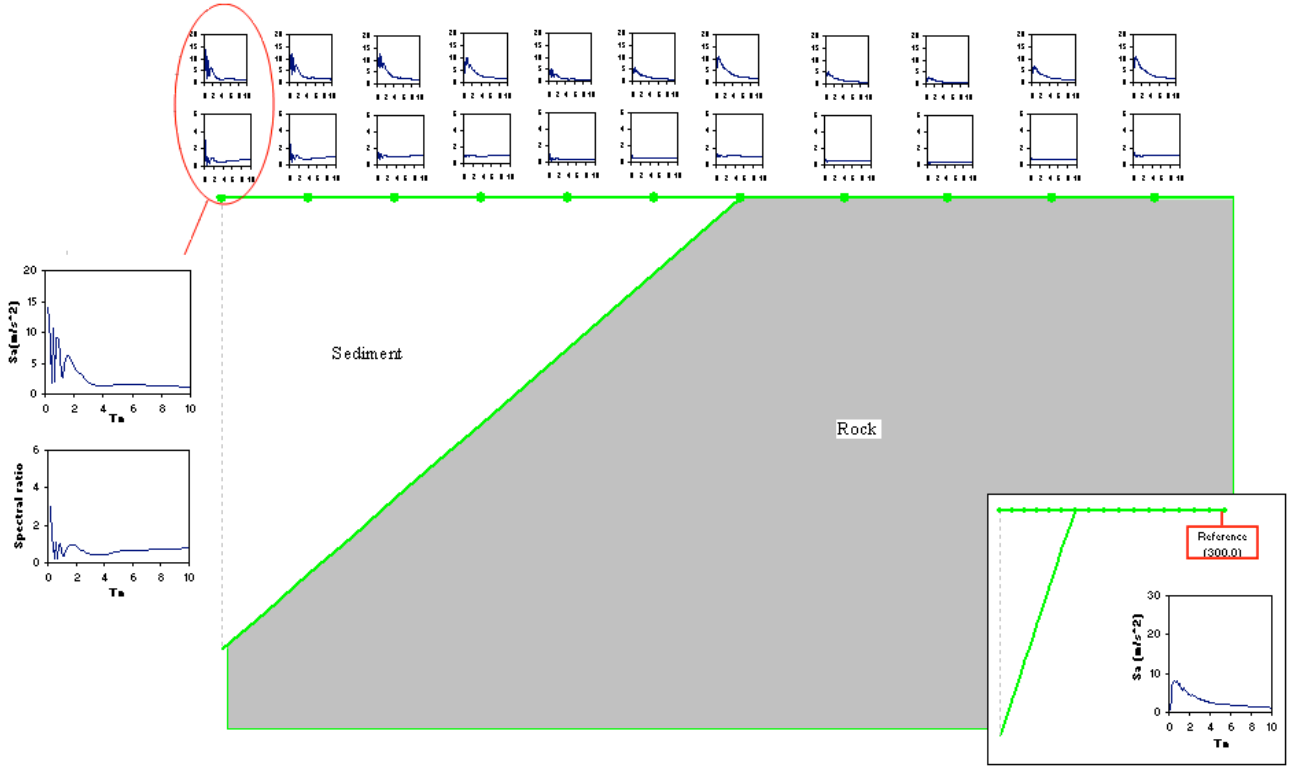
Sa(m/s^2)
Ts
Spectral ratio
Ts
Sediment
Rock
Reference
(300.0)
Sa (m/s^2)
Ts

Table 1

Mechanical parameters for the rock material

	E (MPa)	υ	ρ (kg/m^3)	c (m/s)
rock	6720	0,4	2450	1000

Table 2

Curves classification

Classification	Figure	H/L	Surface (S) m2	Angle (A)	S/A
1	Rectangle	1	20,000	90°	222.2
2	Rectangle	0.6	12,000	90°	133.3
3	Trapezium	1	14,000	120°	116.7
4	Rectangle	0.4	8,000	90°	88.8
5	Triangle	1	10,000	135°	74.07
6	Trapezium	0.6	8,400	135°	62.2
7	Triangle	0.6	6,000	150°	40
8	Trapezium	0.4	5,600	146°	38.4
9	Triangle	0.4	4,000	158°	44.4
10	Rectangle	0.2	4,000	90°	25.3
11	Triangle	0.2	2,000	169°	17.3
12	Trapezium	0.2	2,800	162°	11.8

Table 3

Mechanical parameters of the alluvial layer

	E (MPa)	υ	ρ (kg/m^3)	c (m/s)
soil	900	0,3	1630	465

Table 4

Curves classification

Classification	Figure	H/L	Surface (S) m2	Height (H) m	H/S
1	Rectangle	1	20,000	100	0.005
2	Truncated ellipse	1	15,700	100	0.006
3	Rectangle	0.6	12,000	60	0.005
4	ellipse	1	15,708	100	0.006
5	Truncated ellipse	0.6	9,055	60	0.006
6	Trapezium	0.6	8,400	60	0.007
7	Triangle	0.4	4000	40	0.01